In: *Nonlinear Analysis of Physiological Data*, Edited by H. Kantz, J. Kurths, and G. Mayer–Kress (Springer, Berlin, 1998), pp. 283–306

Human Postural Control: Force Plate Experiments and Modelling

Michael Rosenblum[1,2], Georgy Firsov[2], Robert Kuuz[3], and Bernd Pompe[4]

[1] Max-Planck-Arbeitsgruppe "Nichtlineare Dynamik" an der Universität Potsdam, Am Neuen Palais 19, PF 601553, D-14415 Potsdam, Germany
[2] Mechanical Engineering Research Institute, Russian Academy of Sciences, 101830 Moscow, Russia
[3] Clinic for Nervous Diseases, I. M. Sechenov Moscow Medical Academy, Rossolimo St. 11, Moscow 119021, Russia
[4] Institut für Physik, Ernst-Moritz-Arndt-Universität Greifswald, Friedrich-Ludwig-Jahn-Str. 16, D-17487 Greifswald, Germany

Abstract. We report the results of time series analysis of human body sway while quiet upright stance. The bivariate records (stabilograms) are measured by means of a force plate. To investigate interrelations between oscillations in anterior–posterior and lateral directions we use several techniques: cross-spectrum analysis, generalized mutual information, and calculation of instantaneous relative phase. We find that the stabilograms can be qualitatively rated into two groups: noisy and oscillatory patterns. Further, we show that oscillatory patterns may demonstrate phase locking. We argue that these patterns are due to stochastic and chaotic dynamics, respectively. We discuss the plausible strategy of postural control and present the model that qualitatively describes transitions from noisy to oscillatory patterns and phase synchronization. The relevance of the results of the time series analysis for the diagnostics of neurological pathologies is discussed.

1 Introduction

An important problem in modern neurology is the development of methods for differential diagnostics of various pathologies of the central nervous system (CNS), both of organic and of psychogenic origin. A manifestation of these pathologies are disturbances of posture and locomotion control. On the one hand, quantitative studies of motor control, and equilibrium maintenance in particular, may provide useful diagnostic information on the functional state of the CNS (Gurfinkel et al. 1965; Terekhov 1976; Cernacek 1980; Furman 1994; Lipp and Longridge 1994). On the other hand, investigations of the strategy of the posture control in humans is very interesting from a dynamical standpoint as an example of control in the multi-degree-of-freedom system.

The force plate technique, also known as stabilography or posturography, has been extensively used since decades (Baron 1983) for the analysis of upright postural control and the evaluation of functional states of the human organism. During the tests small sways of the human body in anterior–posterior and lateral directions are measured simultaneously. These records,

called stabilograms, are usually analyzed by means of different statistical techniques, spectral and correlation analysis (Terekhov 1976; Rosenblum and Firsov 1992b; Collins and DeLuca 1994).

In the present paper we describe the results of our force plate investigations of healthy subjects and patients with different neurological pathologies. In our study we concentrate on the joint analysis of both components of the stabilograms. For this purpose we use the standard cross-spectrum analysis technique, the generalized mutual information (Pompe 1993), and the recently found effect of *phase synchronization* of coupled self-sustained chaotic oscillators (Rosenblum et al. 1996; Pikovsky et al. 1996). After the discussion of the plausible strategy of the neural regulation of posture we introduce a model of two–dimensional dynamics of the center of gravity of the body.

2 Experiments

The experiments were accomplished in the Clinic for Nervous Diseases of the Moscow Medical Academy using a standard rigid force plate with four tensoelectric transducers. The output of the setup provides current coordinates (x, y) of the center of pressure under the feet of the standing subject. These coordinates are close to that of the center of gravity of the human body. In the following we denote the deviation of the center of pressure in anterior–posterior and lateral direction as x and y, respectively. Every subject was asked to perform three tests of quiet standing with:

EO — eyes opened and stationary visual surrounding,
EC — eyes closed,
AF — eyes opened and additional video–feedback.

In the AF test the current position of the center of pressure was indicated by a light dot on the screen of an oscilloscope. The subject was instructed to watch the screen and to keep the dot within a circle in its center. The AF test can be considered as a simply realized non-invasive method to change the dynamics of the system in order to extract additional information about it. In all tests the plate was fixed, i.e. no artificial mechanical perturbations of the upright posture were used.

The postural sways have been sampled with a frequency of 25 Hz. Every record contains two channels – each of 4096 points ($\approx$ 160 s). About 150 stabilograms have been obtained testing healthy volunteers and neurological patients. By visual inspection we have rejected some trials, for instance that where the subject moved during the test, or where he or she was not able to stay for three minutes. The later turned out to be rather difficult for patients with a neurological pathology. Thus we got 132 bivariate records which can be considered as free of artifacts. A survey of the data is given in Table1.

Table 1. The subjects under study

#	subject	sex	age	state	group	tests
1 – 3	39	f	23	healthy	1	EO, EC, AF
4 – 6	32	f	23	healthy	1	EO, EC, AF
7 – 9	33	f	25	healthy	1	EO, EC, AF
10 – 12	35	f	26	healthy	1	EO, EC, AF
13 – 15	40	f	27	healthy	1	EO, EC, AF
16 – 18	2	f	31	healthy	1	EO, EC, AF
19 – 21	34	f	32	healthy	1	EO, EC, AF
22 – 24	42	f	36	healthy	1	EO, EC, AF
25 – 27	3	f	37	healthy	1	EO, EC, AF
28 – 30	4	f	40	healthy	1	EO, EC, AF
31 – 33	43	m	22	healthy	1	EO, EC, AF
34 – 36	36	m	25	healthy	1	EO, EC, AF
37 – 39	38	m	21	healthy	1	EO, EC, AF
40 – 42	41	m	22	healthy	1	EO, EC, AF
43 – 45	5	m	27	healthy	1	EO, EC, AF
46 – 48	37	m	27	healthy	1	EO, EC, AF
49 – 51	1	m	29	healthy	1	EO, EC, AF
52 – 54	7	f	26	multiple sclerosis	2	EO, EC, AF
55 – 57	6	f	30	multiple sclerosis	2	EO, EC, AF
58 – 60	30	f	30	multiple sclerosis	2	EO, EC, AF
61 – 63	9	f	42	Parkinson disease	2	EO, EC, AF
64 – 66	10	m	53	Parkinson disease	2	EO, EC, AF
67 – 68	11	m	53	Parkinson disease	2	EO, EC
69 – 71	8	f	62	brain tumor	2	EO, EC, AF
72 – 74	44	m	44	atrophy of cerebellum	2	EO, EC, AF
75 – 77	45	m	54	atrophy of cerebellum	2	EO, EC, AF
78 – 80	46	f	56	discircular encephalopathy	2	EO, EC, AF
81 – 82	47	m	58	discircular encephalopathy	2	EO, EC
83 – 85	12	f	36	neurathenia	3	EO, EC, AF
86 – 88	28	f	42	neurathenia	3	EO, EC, AF
89 – 91	15	f	44	neurathenia	3	EO, EC, AF
92 – 94	27	m	52	hysterical hemiparesis	3	EO, EC, AF
95 – 96	14	f	15	hysterical hemiparesis	3	EO, EC
97 – 99	22	f	20	neurotic disorder	3	EO, EC, AF
100 – 102	25	f	28	neurotic disorder	3	EO, EC, AF
103 – 105	18	f	35	neurotic disorder	3	EO, EC, AF
106 – 108	26	f	40	neurotic disorder	3	EO, EC, AF
109 – 111	23	f	41	neurotic disorder	3	EO, EC, AF
112 – 114	21	f	51	neurotic disorder	3	EO, EC, AF
115 – 117	19	f	51	neurotic disorder	3	EO, EC, AF
118 – 120	24	f	62	neurotic disorder	3	EO, EC, AF
121 – 123	20	f	34	functional ataxia	3	EO, EC, AF
124 – 126	13	f	39	functional ataxia	3	EO, EC, AF
127 – 129	17	f	40	functional ataxia	3	EO, EC, AF
130 – 132	16	f	51	functional ataxia	3	EO, EC, AF

The subjects can be divided first of all into three groups:

Group 1: healthy persons,
Group 2: subjects with an organic pathology (tumor, multiple sclerosis, Parkinson disease),
Group 3: subjects with a psychogenic pathology (neurathenia, functional ataxia).

3 Data Analysis

For the analysis of the stabilograms different methods have already been used, including the calculation of various statistical characteristics – the maximal and root mean square displacement in both directions, the length of the trajectory on the plain, the area inside the contour formed by the trajectory, the calculation and approximation of one and two-dimensional distributions, correlation and spectral analysis, calculation of correlation dimension, and random-walk analysis (Terekhov 1976; Dobrynin et al. 1985; Rosenblum et al. 1989; Rosenblum and Firsov 1992b; Firsov et al. 1993; Collins and DeLuca 1994; Yong 1994).

In the present work we concentrate on the joint analysis of two components of stabilograms. The main question we are trying to answer is: Are the oscillations in anterior–posterior and lateral directions independent or not? To our knowledge, this question has not been systematically addressed in the literature. Our previous study (Rosenblum et al. 1989) showed that the x and y components are linearly uncorrelated if the subject is healthy, and some correlation may appear in pathological case. To clarify this point we use the cross-spectrum analysis and the cross generalized mutual information (GMI). Moreover, we look for synchronization phenomena.

Introducing the Data. Stabilograms appear as some random functions of time (Fig. 1). By visual inspection we can conclude that stabilograms are, as a rule, non–stationary. Further, we can distinguish between noisy and oscillatory patterns, although these notation is to some extend arbitrary. Oscillatory patterns appear considerably less frequently – only some few per cent of the records can be identified as oscillatory. We can also conclude that in our data set the oscillatory patterns appear in pathological cases only. The probability distributions of three records (#1: healthy female, 23 years old, EO; #61: Parkinson disease, 42 years old, EO; and #89: neurathenia, female, 44 years old, EO) are shown in Fig. 2. The histograms of healthy subjects are usually close to Gaussian. Oscillatory patterns, and patterns close to them have the bimodal form of the distribution. We note that in the last record the distribution of x is clearly asymmetrical. Our studies show that this asymmetry is a good indicator of a functional pathology.

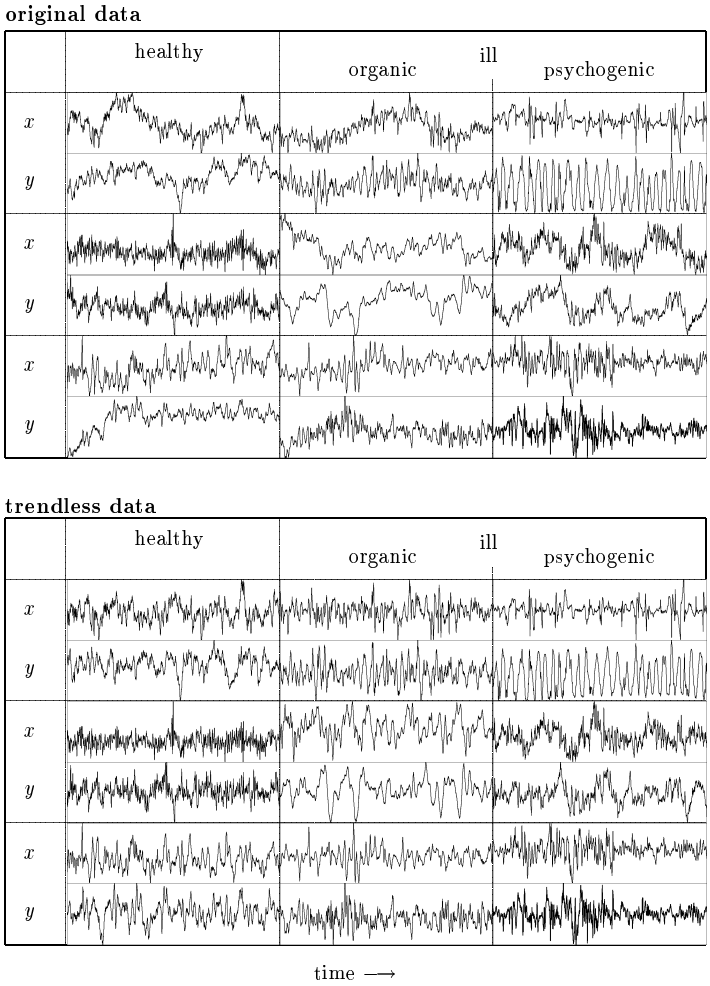

Fig. 1. Typical stabilograms of healthy subjects (records #1, 6, 16, from top to bottom), and patients with organic (records #55, 61, 78) and psychogenic (records #95, 99, 123) diseases. In each signal the time runs from 0 to 164 s

To make the data suitable for our analysis we have removed low-frequency trends. For the cross-spectrum and mutual information analysis it is done by fitting and subtracting a polynomial of order 10. The resulting stationarity of the data was tested with a method proposed elsewhere (Pompe, this volume). The trendless data are shown in the lower panel of Fig. 1. For the calculation of the instantaneous phase the moving average has been subtracted from the data (see below).

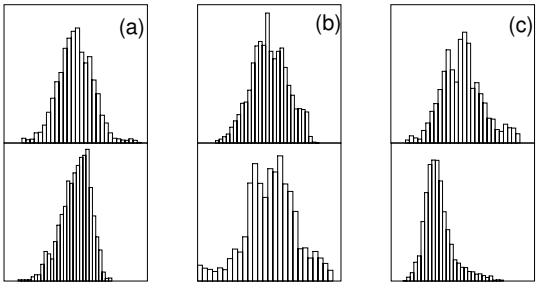

Fig. 2. Probability distributions of stabilograms of a healthy subject, record #1 (a), Parkinsonian patient, #61 (b) and patient with functional ataxia, #89 (c). The upper and low panels show the distributions for x and y

Linear Analysis. A standard technique to analyze the linear relationships between two signals leads to the cross-spectrum $S_{xy}(f)$ of the processes x and y. It is defined as the Fourier transform of their cross-correlation function. For the quantification of linear correlations in the frequency domain the *coherence function* $\gamma^2(f)$ is used:

$$\gamma^2(f) = \frac{|S_{xy}(f)|^2}{S_x(f)S_y(f)} \ , \tag{1}$$

where S_x and S_y are the auto–spectra of x and y, respectively. The coherence function varies from 0 to 1. The lower bound corresponds to the case where the frequency components of both signals are linearly independent whereas in all other cases linear relationships are indicated. Another important characteristic is the *phase spectrum*

$$\psi(f) = \arg S_{xy}(f) \ . \tag{2}$$

It represents the phase shift between frequency components, provided they are coherent. Otherwise it has no meaning. In our calculations we use the following parameters: the original record is divided in 12 overlapping samples of 1024 points each and the result is obtained by averaging over 12 periodograms using the Bartlett window.

The power spectra of noisy stabilograms decay monotonically, and the coherence functions γ^2 are considerably less than unity for the whole frequency range (Fig. 3). This indicates the absence of linear correlations between x and y. Although some broad peaks appear in the spectra of the y components in Fig. 3, no significant coherence is seen. In some cases coherence can be observed in the frequency range of the so-called θ-rhythm of corresponding electroencephalograms (4–6 Hz). This may indicate certain intellectual

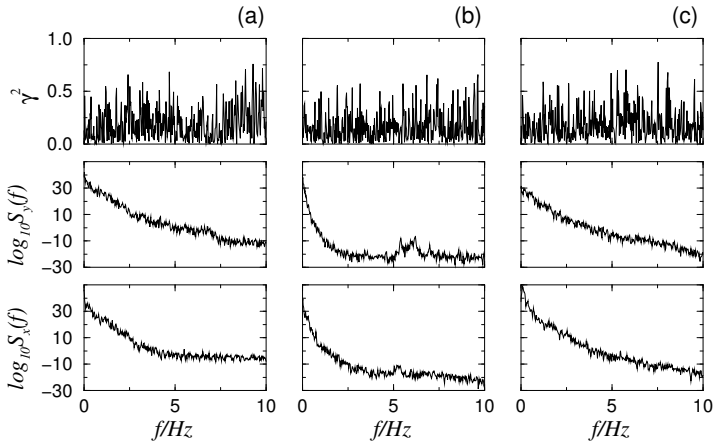

Fig. 3. Typical cross-spectrum of the stabilogram of a healthy subject (record #4) (a) and cross-spectra of Parkinsonian patient (record #61) (b) and the subject suffering from neurathenia (record #89) (c). From bottom to top are shown: the auto-spectra of x and y, and the coherence function γ^2 of the the cross-spectrum. (b): There is some significant increase of the spectral density around 6Hz, but the x and y oscillations are not coherent. Nevertheless, significant dependencies between components of the stabilogram can be revealed by nonlinear techniques (see below)

or emotional stress (Fig. 9c). The results of the linear analysis are summarized in Fig. 4, where the coherence functions are shown for all 132 records as a gray scale picture. The white and full black level corresponds to $\gamma^2 = 0$ and $\gamma^2 = 1$, respectively. We can conclude that with the exception of some pathological records the components of stabilograms are noncoherent.

Analyzing Nonlinear Dependencies in the Data. In order to reveal the presence or absence of dependencies between the postural control signals $y(t)$ and $x(t+\tau)$ we consider the cross mutual information $I_\varepsilon(\tau)$ of them. It represents the mean (over all instants t) information we get from $y(t)$ on $x(t+\tau)$ and vice versa. The parameter $\varepsilon > 0$ denotes the relative level of coarse graining, $\varepsilon \ll 1$. For smaller values of ε more details of the relation between the signals can be detected, however, the reliability of the estimates is decreased in this way. Here we have chosen $\varepsilon = 0.05$ which means that we consider each signal with a precision of 5 % of its total variation range. The time lag τ is taken as the independent variable leading to the mutual information function. It can be considered as a nonlinear analogon to the squared correlation function. In our applications τ runs in an interval around zero (-10 s $< \tau <$ 10 s). For $\tau \to \pm\infty$ the mutual information typically vanishes reflecting the absence of long term relations of the posture control

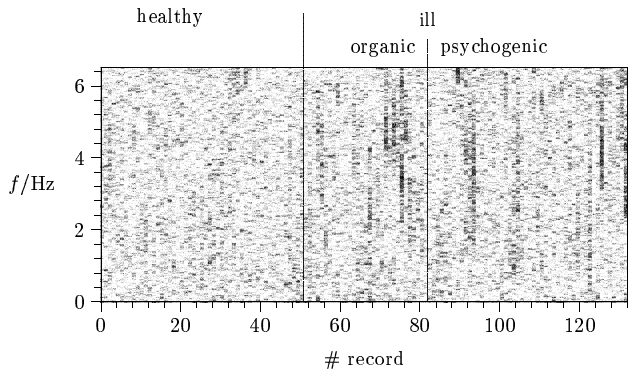

Fig. 4. Coherence functions $\gamma^2(f)$ of of 132 bivariate postural control records $[x(t), y(t)]$ of healthy and ill subjects

data.

We present results for the so-called *generalized mutual information* (GMI). It causes some computational efforts in comparison to the usual Shannonian mutual information. For each τ the GMI fulfills the relations

$$0 \leq I_\varepsilon(\tau) \leq -\log_2 \varepsilon \approx 4.32\,\text{bit} \ .$$

Their interpretation is as follows: The quantities $y(t)$ and $x(t+\tau)$ can be considered as independent within all accuracy levels $\geq \varepsilon$ if and only if $I_\varepsilon(\tau) = 0$. On the other hand, $x(t+\tau)$ follows uniquely from $y(t)$, within the relative accuracy ε, if and only if $I_\varepsilon(\tau)$ attains its upper bound $-\log_2 \varepsilon$. The larger $I_\varepsilon(\tau)$ the stronger are the linear and nonlinear statistical relations between $y(t)$ and $x(t+\tau)$. Here we work with trendless data – stationarity is crucial for the GMI estimations. A more detailed description of the method is given elsewhere (Pompe, this volume).

We have calculated the GMI function for each of the 132 bivariate records (x, y) of Table 1. In Fig. 5a the functions are encoded by a gray scale and plotted vertically – horizontally the number of the record runs. The GMI functions vary between 0 and 1 bit corresponding to a range of $0 \ldots 23\%$ of the maximum possible information of about 4.32 bit. In most cases $I_\varepsilon(\tau)$ lies in the range 0.25 ± 0.2 bit indicating that the dependencies are rather week. This is true for healthy as well as for ill subjects. However, in the later case we sometimes observe relatively strong dependencies over a wide range of time lags τ, for instance for the records #61–63 corresponding to a person suffering from the Parkinson disease. (The bivariate record #61 is shown in Fig. 1.) It is important to underline that the cross-spectral analysis shows no coherence for this record (see Fig. 3b) whereas the analysis of the relative phase also shows strong interrelations between x and y.

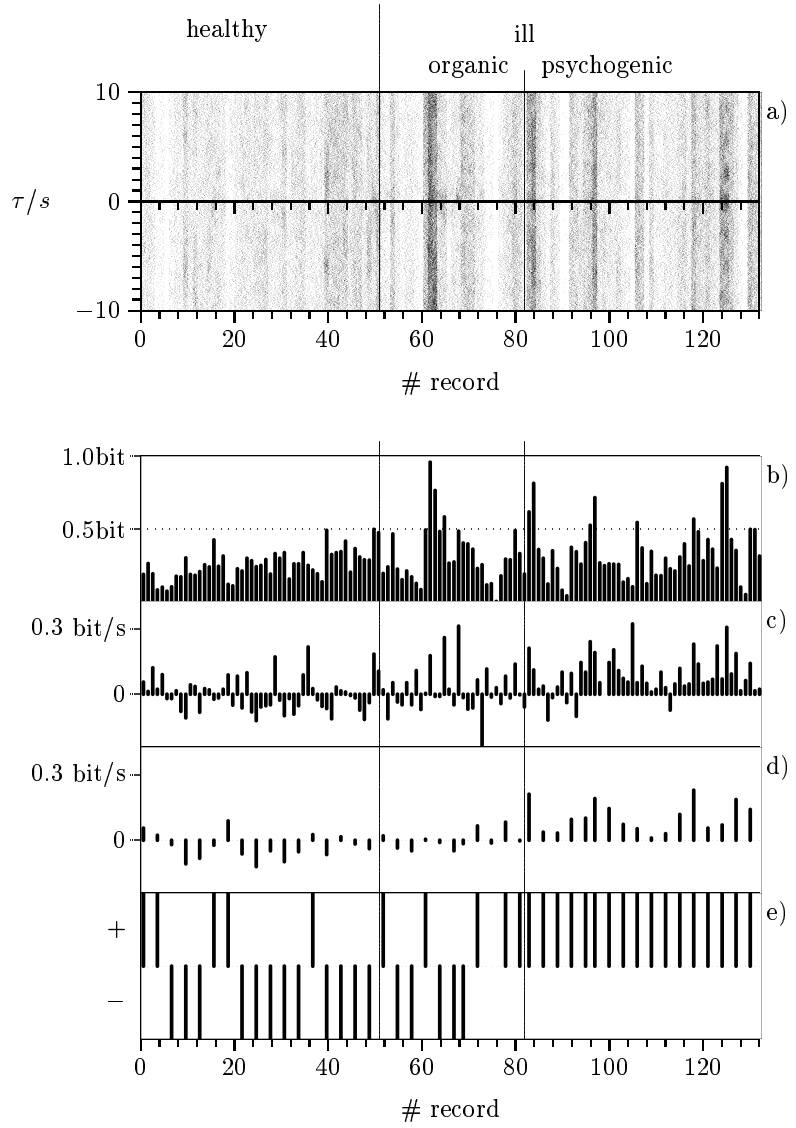

Fig. 5. In (a) the cross mutual information functions $I_\varepsilon(\tau)$ of 132 bivariate postural control records $[x(t), y(t)]$ of healthy and ill subjects are represented. Strong dependencies between $y(t)$ and $x(t+\tau)$ correspond to the more dark regions. The diagrams (b)–(e) represent features extracted from the mutual information functions:
(b) mean of $I_\varepsilon(\tau)$ for $-0.5\text{s} < \tau < 0.5\text{s}$,
(c) decay of $I_\varepsilon(\tau)$ for $\tau = 0 \to 0.5\text{s}$ and $\tau = 0 \to -0.5\text{s}$,
(d) the same as in (c) but only records where the subject had eyes opened,
(e) the same as in (d) but indicating only the sign

From the representation in Fig. 5a we cannot well discriminate between healthy and ill subjects. Nevertheless, the situation improves if we investigate the GMI functions for small values of the time lag, say $-1\ \mathrm{s} \lesssim \tau \lesssim 1\ \mathrm{s}$. In this region we can derive from the functions several features which have some discriminating power. Figures 5b–e give several examples.

In Fig. 5b the mean of the mutual information for small time lags is represented. It is defined as

$$\frac{1}{2\Delta\tau}\int_{-\Delta\tau}^{\Delta\tau} I_\varepsilon(\tau)\,\mathrm{d}\tau \quad . \tag{3}$$

For about 15 % of the records of the ill subjects this mean is larger than the corresponding largest value of the healthy subject which are the outliers (records # 40, # 50, and # 51). From the figure we can conclude that the x–y-coupling is more likely to be stronger for ill subjects. If the mean mutual information exceeds the threshold of 0.5bit $\approx 0.11 \times \log_2 \varepsilon^{-1}$ then it is very likely that the person is ill. We get nearly the same figure by deriving the mean according to (3) for any $\Delta\tau$ =0.2–2 s. Moreover, it should be noted that this analysis is done with ranked data (Pompe, this volume). All this makes the discrimination rather robust.

In Fig. 5c the mean decay of $I_\varepsilon(\tau)$ for small time lags is plotted. We define it as

$$\mathrm{feature}_1 \equiv \frac{2 \times I_\varepsilon(0) - I_\varepsilon(-\Delta\tau) - I_\varepsilon(\Delta\tau)}{\Delta\tau} \quad . \tag{4}$$

From the figure we conclude that for subjects suffering from a psychogenic disease it is rather likely that this quantity is positive indicating that there is a decrease of the x–y-coupling for growing absolute time lags. If there is no such coupling at $\tau \approx 0$ then the decay of $I_\varepsilon(\tau)$ is mainly determined by random fluctuations of the estimator of $I_\varepsilon(\tau)$. This leads first of all to the somewhat random fluctuations of the corresponding feature of the healthy subjects.

In Fig. 5d the same as in Fig. 5c is shown, but now only the results for the EO test are plotted. For ill persons we often get positive values whereas for healthy subjects negative values seem to be somewhat more likely. For subject with a psychogenic disease this is most striking as it becomes obvious from the plot of the sign in Fig. 5e.

The same investigations were done for the squared cross correlation instead of the GMI functions. The results are presented in Fig. 6. A comparison with Fig. 5 shows that we could expect better distinctive marks from the nonlinear analysis of the data in Fig. 5.

We have done some more attempts to find distinctive marks from the GMI functions. For instance, we also considered higher order cross GMI functions $I_{\varepsilon,\vartheta}(\tau)$ describing relations between $[y(t-\vartheta), y(t)]$ and $x(t+\tau)$, $\vartheta > 0$. In general, the additional knowledge of $y(t-\vartheta)$ cannot decrease the information on $x(t+\tau)$. Indeed, in our numerical experiments we always found an increase

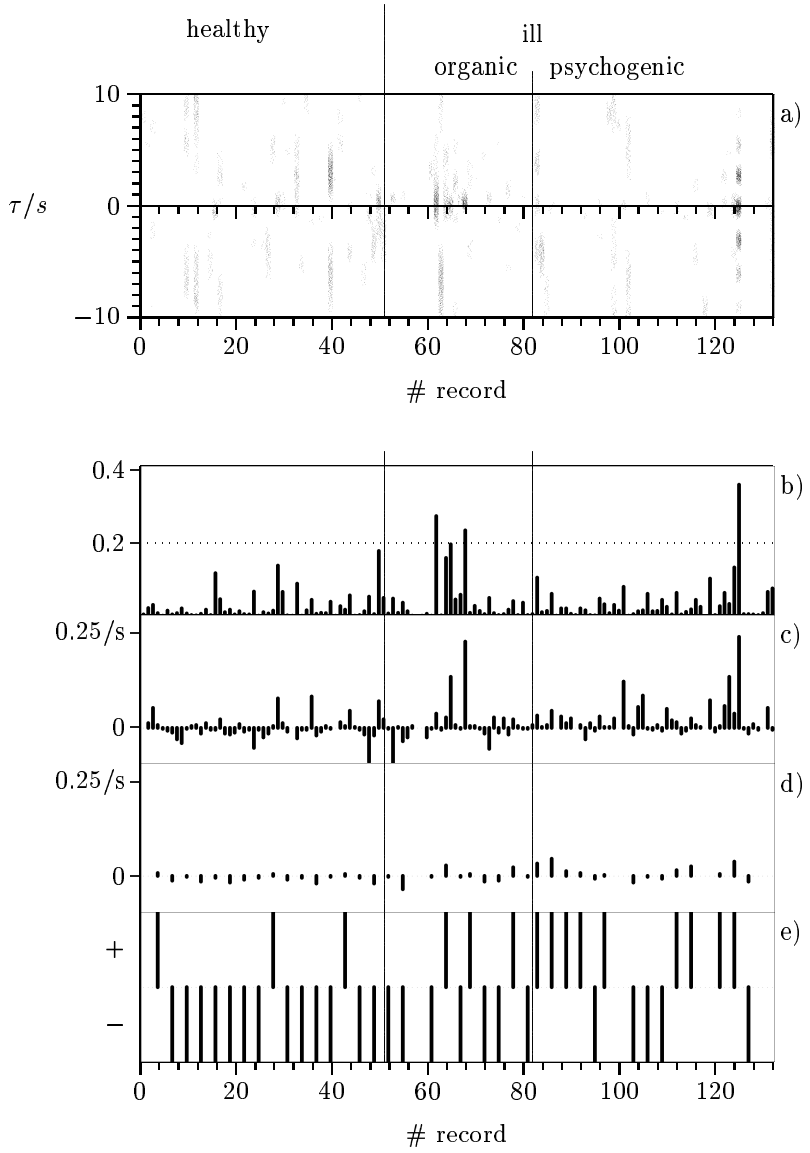

Fig. 6. In (a) the squared cross correlation functions $\varrho^2(\tau)$ of 132 bivariate postural control records $[x(t), y(t)]$ of healthy and ill subjects are represented. Strong correlations between $y(t)$ and $x(t+\tau)$ correspond to the more dark regions. The diagrams (b)–(e) represent features extracted from the squared correlation functions:
b: mean of $\varrho^2(\tau)$ for $-0.5\text{s} < \tau < 0.5\text{s}$,
c: decay of $\varrho^2(\tau)$ for $\tau = 0 \to 0.5\text{s}$ and $\tau = 0 \to -0.5\text{s}$,
d: the same as in (c) but only records where the subject had eyes opened,
e: the same as in (d) but only indicating only the sign

of this information which was somewhat larger for ill subjects. Thus we are inclined to define another feature

$$\text{feature}_2 \equiv \frac{1}{2\Delta\tau} \int_{-\Delta\tau}^{\Delta\tau} [I_{\varepsilon,\vartheta}(\tau) - I_{\varepsilon}(\tau)]\, \mathrm{d}\tau \ . \tag{5}$$

Figure 7 represents a plot of feature_2 against feature_1. Almost all feature vectors of healthy subjects are found within the circle whereas that of about 80% of the ill subjects are outside. The discrimination is a bit more striking for subjects suffering from a psychogenic disease.

In our calculations we have chosen $\Delta\tau \approx 0.5\,\text{s}$ and $\vartheta = 40\,\text{ms}$. However, any $\Delta\tau = 0.2$–2 s and $\vartheta = 40$–250 ms would provide a rather similar discrimination of $70 \ldots 80\%$.

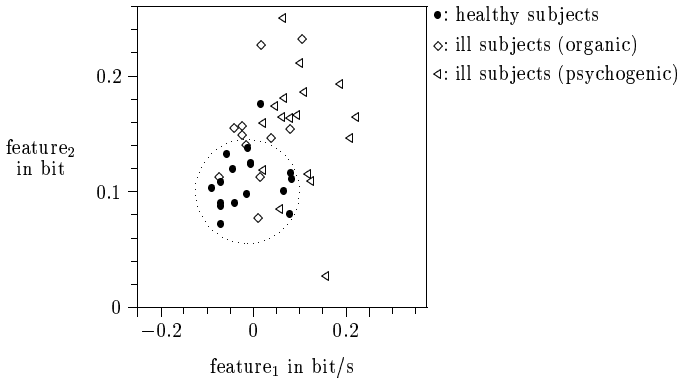

Fig. 7. Plot of two characteristic features of the cross generalized mutual information functions of the postural control data recorded with opened eyes. The feature_1 is defined in (4). It describes the decay of the x–y-coupling for increasing time lag. The feature_2 is defined in (5). It describes the increase of the coupling by an additional coordinate

Our investigations suggest that we could derive some characteristic parameters describing the nonlinear relationship between the postural control data and having some discriminating power between healthy and ill subjects. This might be important for medical diagnosis. However, more data records are needed to get more reliable statements.

Search of Phase Synchronization. To analyze oscillatory patterns we calculate *instantaneous phases* ϕ_1 and ϕ_2 of the signals x and y using the Hilbert transform. An introduction of this technique is given elsewhere (Rosenblum

and Kurths, this volume). If the relative phase $\Delta\phi = \phi_1 - \phi_2$ is limited, the presence of phase synchronization of interacting chaotic oscillators may be indicated (Rosenblum et al. 1996; Pikovsky et al. 1996). Possible models of the underlying dynamics are discussed below. We underline that the method is suitable for processing non-stationary data, and it can reveal alternating epochs of qualitatively different behavior. Applications of this method to the analysis of the cardiorespiratory system of a piglet are presented elsewhere (Hoyer et al., this volume).

In order to eliminate low-frequency trends, the moving average computed over the n-point window was subtracted from the original data. The window length n has been chosen by trial to be equal or slightly larger than the characteristic oscillation period. Its variation up to two times does not practically effect the results.

Here we present in detail results of the analysis of several records. For the first example stabilograms of a female subject were investigated (records #124–126: 39 years old, functional ataxia). We can see that in the EO and EC test the patterns are clearly oscillatory (Fig. 8). The difference between these two records is that with eyes opened the oscillations in two directions are not synchronous during approximately the first 110 s, and are phase locked during the last 50 s. In the EC test, the phases of oscillations are perfectly entrained during all the time. In both cases the phase difference fluctuates around zero (the mean value $\langle\Delta\phi\rangle \approx 0.003$). From the power cross-spectra (Fig. 9) we see that, although the low-frequency peaks are clearly seen, the coherence is not very high ($\gamma^2 \approx 0.5$ for the EO test and $\gamma^2 \approx 0.7$ for the EC test), as well as the maximal value of the GMI function ($I_\varepsilon(\tau) < 0.2 \times \log_2 \varepsilon^{-1}$ for the EO test and $I_\varepsilon(\tau) < 0.23 \times \log_2 \varepsilon^{-1}$ for the EC test). The behavior is essentially different in the AF test. The patterns become more noisy and no phase locking or increased coherence in the low-frequency domain is observed. Instead of it, the coherence is increased in a rather broad frequency range ($\approx$ 3–5 Hz) which is close to the frequency of the θ-rhythm in EEG. Such qualitative changes of dynamics (from oscillatory to noisy) was several times observed for psychogenic patients. Further investigations are required in order to find out whether this test can be used as a diagnostic tool.

For the second example we have chosen the stabilogram of a Parkinsonian patient (records #61–63: female, 42 years old). During the EO test both 1:1 and 1:2 synchronous epochs can be found (Fig. 10), although the second one is rather short (about 10 seconds). It is important to notice that in the 1:1 regime the phase difference is significantly non-zero ($\langle\Delta\phi\rangle \approx 0.4$ in the interval 70–100 s and $\langle\Delta\phi\rangle \approx -0.7$ in the interval 100–130 s). During the EC test only an 1:2 phase locking epoch of about 50 s was observed (Fig. 11). No synchronization was found for the AF test.

We underline that the fact that both components of the stabilogram can be rated as oscillatory patterns does not mean the occurrence of the synchro-

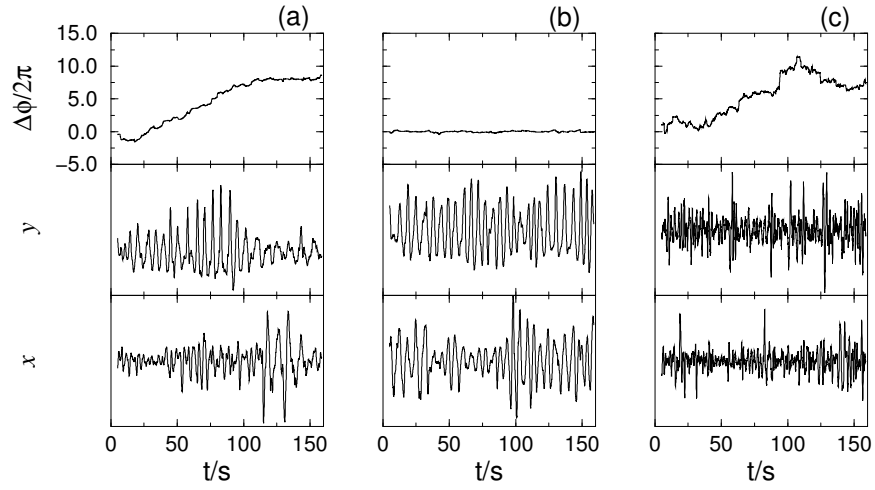

Fig. 8. Stabilograms of an ataxia patient (records #124–126) after trend elimination for EO (a), EC (b), and AF (c) tests. The upper panels show the relative phase between two signals x and y. During the last 50s of the first test and the whole second test the phases are perfectly locked. No phase entrainment is observed in the AF test

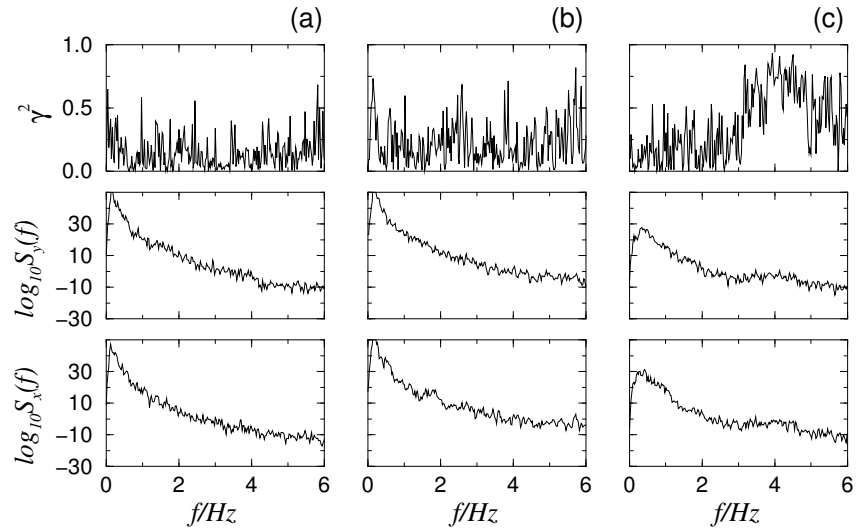

Fig. 9. Auto-spectra and coherence functions for the stabilograms shown in Fig. 8. Although the time series in the EC tests are perfectly phase locked, the spectral analysis shows no significant coherence

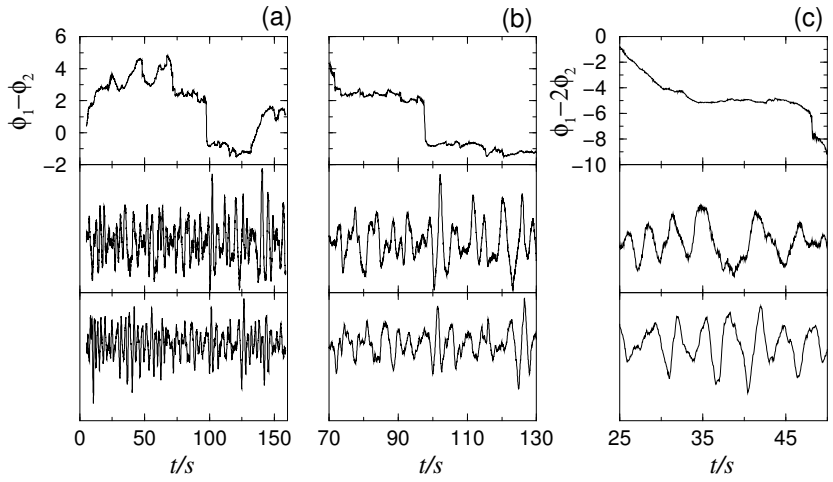

Fig. 10. Stabilogram of a Parkinsonian patient (record #61) after trend elimination for the EO test. The upper panels show the relative phase between two signals x and y. Enlarged parts of (a) show epochs of 1:1 (b) and 1:2 (c) locking

nization. Thus, the patient with the tumor has shown oscillatory patterns in all three tests but no synchronization was found.

4 Model of Postural Control Dynamics

Several mathematical models of posture dynamics have been proposed in the literature. All of them consider only one-dimensional sways of the center of gravity of the human body. The muscle–skeleton subsystem is represented as one-link (Aggashjan and Palcev 1975; Matsushira et al. 1983; Rosenblum et al. 1989) or multi-link inverted pendulum (Rosenblum and Firsov 1992a), or considered as a pinned polymer (Chow and Collins 1995). The crucial point is modelling the control subsystem, i.e. the regulating functions of the CNS. The structure of this system and strategy of the control are highly complicated. Nevertheless, several main principles can be outlined:

- The CNS realizes simultaneously feedforward and feedback control. This provides high reliability of the whole system. The controlled variables are, respectively, stiffness of the joints and elastic torques. These variables are governed by separate cortical systems and adjusted via coactivation and reciprocal activation of muscles (Humprey and Reed 1983).
- The CNS constantly receives information on angles and angular velocities of joints. This information is provided by *proprioceptors*, visual and vestibular analyzers. The main role is played by proprioceptors. Experimental

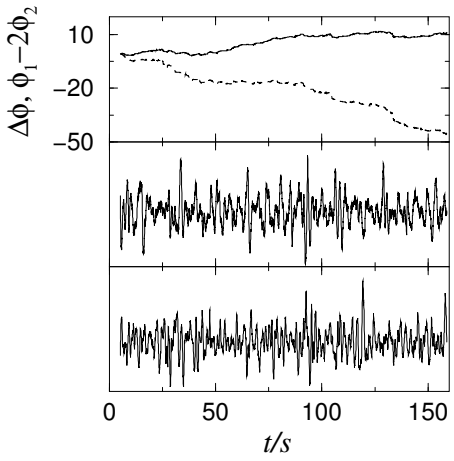

Fig. 11. Stabilogram of an Parkinsonian patient (record #62) after trend elimination for the EC test. The upper panels show the relative phase $\Delta\phi = \phi_1 - \phi_2$ between the signals x and y (solid line) and $\phi_1 - 2\phi_2$ (dashed line). 1:2 phase locking is seen in the time interval 40–90 s.

studies confirm that the nervous system constantly uses this information for the maintenance of posture (Gurfinkel et al. 1982, Litvincev and Tur 1988).

- The characteristics of the proprioceptors (in the muscles and joint spindles, tendon receptors) are essentially nonlinear. Namely, there exist some *sensibility thresholds* which were directly measured in physiological experiments (Gurfinkel et al. 1982). The existence of these thresholds was also indirectly confirmed by results of time series analysis (Collins and De Luca 1994).
- The important property of the feedback loops is time delay caused by the finiteness of the velocity of propagation and processing of the information in the nervous system. The value of the delay is estimated as 0.1–0.8 s (Gurfinkel et al. 1965, Williams 1981).

4.1 Modelling One–Dimensional Sways

The first model of posture dynamics was proposed in (Aggashjan and Palcev 1975) in the form of an one–link inverted pendulum elastically linked to the base

$$\ddot{\varphi} + 2h\dot{\varphi} + \omega^2\varphi + R = \xi(t) \ . \tag{6}$$

$\xi(t)$ is "white" Gaussian noise, and R denotes the regulating action of the CNS. It was assumed that the control is based on position and velocity feedback loops with time delay, $R = c_1\varphi(t-\tau) + c_2\dot{\varphi}(t-\tau)$. Thus, the origin of

the body sway while quiet standing was supposed to be a result of fluctuations in the control and mechanical subsystems. A similar model was studied in (Matsushira et al. 1983). To account for the sensibility threshold of proprioceptors, Matsushira et al. have also considered piecewise linearity in the feedback loop. They found that this leads to the excitation of periodic oscillations corrupted by noise.

The importance of the nonlinearity in the feedback loops was demonstrated elsewhere (Rosenblum et al. 1989, Rosenblum and Firsov 1992a). The following model was studied numerically (Fig. 12a):

$$\ddot{\varphi} + 2h\dot{\varphi} + \omega^2\varphi + c_1\mathcal{F}\big(\varphi(t-\tau), \lambda_1\big) + c_2\mathcal{F}\big(\dot{\varphi}(t-\tau), \lambda_2\big) = 0 \ , \qquad (7)$$

where the piecewise linear function $\mathcal{F}$ describes the characteristics of the proprioceptors with sensitivity thresholds $\lambda_{1,2}$,

$$\mathcal{F}(x, x_0) = (x - x_0)\Theta(x - x_0) + (x + x_0)\Theta\big(-(x + x_0)\big) \ , \qquad (8)$$

$\Theta(\cdot)$ is the Heaviside step function. For this model in a broad range of parameters chaotic oscillations arise. It was concluded that oscillations of the center of gravity of the human body may be of deterministic origin.

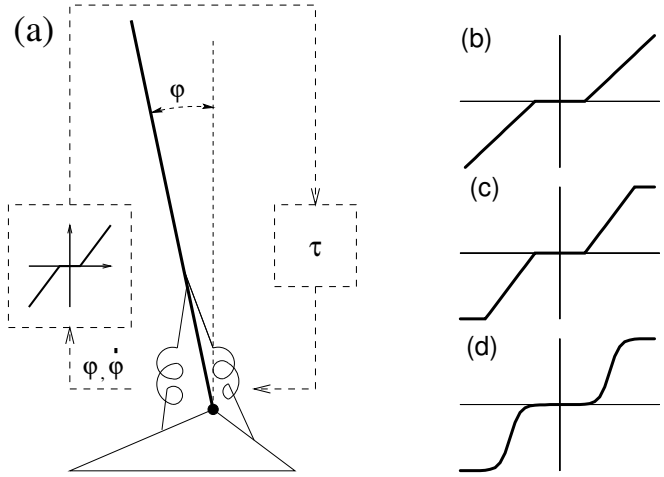

Fig. 12. Scheme of the one-link inverted pendulum model (a). The dashed line denotes the feedback loop with time delay τ. The nonlinear properties of proprioceptors are modelled by a piecewise linear functions (b), (c) or smooth function (c).

Another model (Rosenblum and Firsov 1992a) was proposed on the base of the so-called *equilibrium point hypothesis* (Feldman 1979; Hogan 1985).

According to this hypothesis the muscle–skeleton subsystem is considered as a mass–spring system where the lengths and elasticities of the springs are adjusted by the controller (CNS). Hence, the CNS defines the equilibrium configuration, or state, of the system (in the one-dimensional case we can speak about the equilibrium point). In the process of movement the CNS changes the equilibrium point and the mechanical system goes to this new equilibrium state according to general mechanical laws and in spite of small external perturbations. The control of movements in the presence of rapid external perturbations is mainly achieved by an increase of the stiffness of the joints. The constant posture is maintained by means of shifting the equilibrium point while the stiffness can be considered constant (Humprey and Reed 1983).

Let us denote the coordinate of the center of gravity by x and consider small oscillations in the vicinity of the equilibrium point z,

$$\ddot{x} + 2h\dot{x} + \omega^2(x - z) = 0 \ . \tag{9}$$

The CNS regulates the posture moving the equilibrium point. This regulation is based (a) on the information on x and its derivative that is obtained with some time delay, and (b) information on the current equilibrium state "known" to the controller. Hence, we can write

$$\dot{z} = f\big(z, x(t-\tau_1), \dot{x}(t-\tau_2), \dots\big) \ .$$

As the first approximation we take

$$\dot{z} = -\tilde{c}_0 z - \tilde{c}_1 \mathcal{F}\big(x(t-\tau), \lambda_1\big) - \tilde{c}_2 \mathcal{F}\big(\dot{x}(t-\tau), \lambda_2\big) \ , \tag{10}$$

where $\mathcal{F}$ is the characteristic of proprioceptors. If $\tilde{c}_0 \gg h$, (9) and (10) reduce to (7) with the feedback coefficients $c_{1,2} = \omega^2 \tilde{c}_{1,2}$. Simulations of the model (9), (10) on the one hand and (7) on the other hand give qualitatively similar results.

The models described above can be divided into two groups: the models of Aggashjan and Palcev 1975, and Matsushira et al. 1983 imply that stabilograms originate from some fluctuations, whereas the models of Rosenblum et al. 1989, and Rosenblum and Firsov 1992a are purely deterministic. The stabilograms are rather short and it is impossible to get considerably longer records even with healthy subject (the tests are rather tiresome). That is why we believe that the identification of the origin of the body sway ("noise versus chaos") on the basis of time series analysis is hardly possible. Nevertheless, the approximately $1/f$ behavior of power spectra of some of the noisy patterns can be considered as a hint (but certainly not as a proof) that the body sways are caused by some fluctuations. Contrary to that, the appearance of oscillatory patterns suggests self-oscillation excitation.[1] More

[1] Although the periodic-like oscillations may appear as a result of filtration of some noise, it seems to be rather unlikely that the control system acts like such a narrow-band filter.

strong evidence of deterministic dynamics, although certainly noisy, is the occurrence of phase synchronization which is a characteristic feature of interaction between self–sustained oscillators. Therefore, we assume that both noise and chaos can be responsible for the observed phenomena. Hence, in modelling we take into account both stochastic and deterministic origin of oscillations under study. Namely, we consider the following model:

$$\ddot{\varphi} + 2h\dot{\varphi} + \omega^2\varphi + c_1\mathcal{F}\big(\varphi(t-\tau), \lambda_1\big) + c_2\mathcal{F}\big(\dot{\varphi}(t-\tau), \lambda_2\big) = \xi(t) \ , \qquad (11)$$

where the characteristics of proprioceptors are described by a piecewise linear or smooth nonlinear function $\mathcal{F}$. $\xi(t)$ is some noise which is taken to be white and Gaussian. We have simulated (11) for three different functions $\mathcal{F}$ (Fig. 12b–d) and have not found essential dependencies of the results on the choice of the function. In further examples we use the function plotted in Fig. 12c. In the purely deterministic case ($\xi(t) = 0$) we found periodic, chaotic, and decaying (transient) solutions depending on the parameter values.[2]

An interesting feature of the system (11) is its response to noisy forcing. Besides "trivial" behavior (random oscillations in the vicinity of the stable equilibrium point that can be considered as a model of noisy patterns Fig. 13a), we have observed the following: Small noise can induce the appearance of a structure in the phase space that is reminiscent to the strange attractor which exists in the phase space of the dynamical system for close parameter values. Alternatively, for the parameter values corresponding to the existence of the limit cycle in the noise-free system, the noise not just corrupts the cycle but makes it very similar to the strange attractor (Fig. 13b, c). As a result, the parameter region corresponding to irregular periodic–like oscillations (that are either noisy chaotic or noisy periodic) is rather broad.

To summarize, the proposed model describes qualitatively the appearance of noisy and oscillatory patterns – forced random oscillations and chaotic self-oscillations disturbed by noise, respectively. The sensitivity thresholds $\lambda_{1,2}$ and the coefficients $c_{1,2}$ may serve as the physiologically relevant bifurcation parameters.

4.2 Modelling Sways in Two Dimensions

From the fact that body sways of healthy persons in anterior–posterior and lateral directions are independent, we can conclude that there exist two separate control systems governing maintainance of the upright posture. We assume that both systems can be described by equations of the form (11).

[2] If the proprioceptor characteristics of Fig. 12b is used, infinitely growing unstable solutions may occur. As we restrict ourselves to modelling small oscillations around the equilibrium, we do not consider these solutions. We do not perform the detailed bifurcation analysis of the model because there are 6 free parameters, and the physiological meaning of two of them, $c_{1,2}$, is not clear.

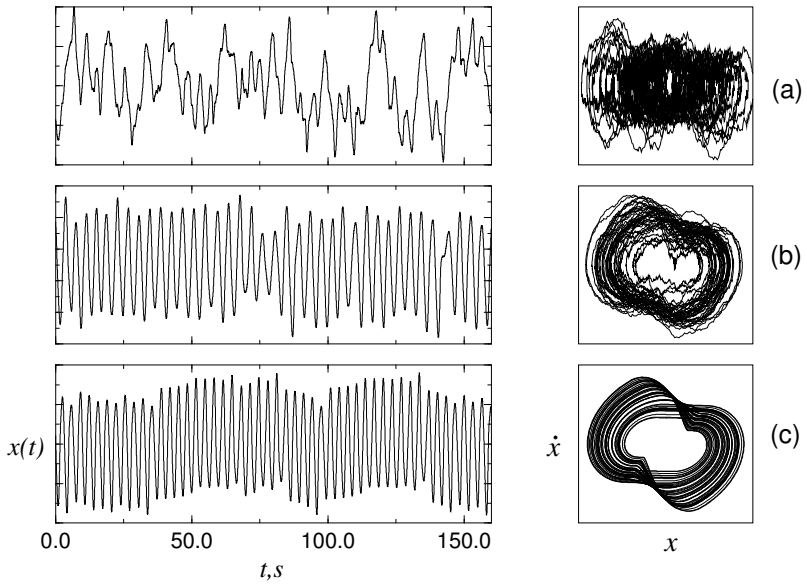

Fig. 13. Simulated time series $x(t)$ (left column) and projections of the corresponding attractors on the plane $x, \dot{x}$ (right column). (a) Simulated noisy pattern ($\lambda_1 = \lambda_2 = 0.01$, $c_1 = 4$, $c_2 = 8$, $\sigma_\xi = 0.1$). (b) Oscillatory pattern ($\lambda_1 = 0.01$, $\lambda_2 = 0.05$, $c_1 = 4$, $c_2 = 8$, $\sigma_\xi = 0.1$). In the absence of noise the attractor of the system is the limit cycle. Influence of noise results in the structure similar to the attractor of the noise–free system for close parameter values (cf. (c)). (c) Chaotic solution ($\lambda_1 = 0.01$, $\lambda_2 = 0.05$, $c_1 = 7$, $c_2 = 8$, $\sigma_\xi = 0$)

Of coarse, the parameters of these equations can differ. In the following we suppose that the time delay τ is the same for both systems because it is determined by the length of the neural fibers and the velocity of the signal propagation. These parameters are likely to be equal for both systems.

As the results of the data analysis show, there are several qualitatively different situations:

1. The x and y are noisy-like. No synchronization was observed in such a case.
2. Both x and y are oscillatory-like and may be either synchronous (with different relation of frequencies) or not. Moreover, synchronous and non-synchronous epochs may alternate within one test.
3. Intermediate situations are also possible – one component is noise-like and another is oscillatory-like. No synchronization is found in this case.

The first and third case can be easily modelled by two equations of the form (11) with two independent noise sources ξ and η. The appearance of the phase

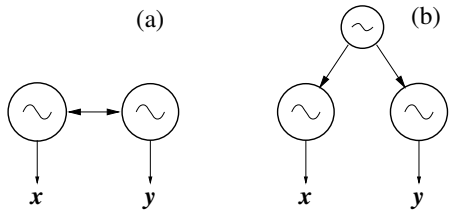

Fig. 14. Two possible oscillatory structures explaining the observed effect of phase synchronization: two coupled self-oscillatory systems (a) and two self-oscillators entrained by the common external driving. In both cases signals x and y may demonstrate phase locking

locking can be explained in different ways:

- Due to some coupling between two chaotic oscillators they can synchronize (Fig.14a). This situation can be described by the following model:

$$\begin{aligned} \ddot{x} + 2h_x\dot{x} + \omega_x^2 x + c_{x,1}\mathcal{F}\big(x(t-\tau),\lambda_{x,1}\big) + c_{x,2}\mathcal{F}\big(\dot{x}(t-\tau),\lambda_{x,2}\big) = \\ \varepsilon_x(\dot{y}-\dot{x}) + \xi(t) \ , \\ \ddot{y} + 2h_y\dot{y} + \omega_y^2 y + c_{y,1}\mathcal{F}\big(y(t-\tau),\lambda_{y,1}\big) + c_{y,2}\mathcal{F}\big(\dot{y}(t-\tau),\lambda_{y,2}\big) = \\ \varepsilon_y(\dot{x}-\dot{y}) + \eta(t) \ , \end{aligned} \tag{12}$$

  where $\varepsilon_{x,y}$ are the coupling coefficients. The coupling between two control systems may arise, e.g., due to some abnormal function of neural processing making the information from two different channels mutually redundant. The results of the simulation are presented in Fig. 15a.
- If the oscillations excited in two control systems are entrained by some external oscillatory source their phases are also locked (Fig.14b). This external source may appear due to some pathological excitation in the brain, e.g., in the case of Parkinsonian disease. The appropriate model can be written as

$$\begin{aligned} \ddot{x} + 2h_x\dot{x} + \omega_x^2 x + c_{x,1}\mathcal{F}\big(x(t-\tau),\lambda_{x,1}\big) + c_{x,2}\mathcal{F}\big(\dot{x}(t-\tau),\lambda_{x,2}\big) = \\ \varepsilon_x \sin\Omega t + \xi(t) \ , \\ \ddot{y} + 2h_y\dot{y} + \omega_y^2 y + c_{y,1}\mathcal{F}\big(y(t-\tau),\lambda_{y,1}\big) + c_{y,2}\mathcal{F}\big(\dot{y}(t-\tau),\lambda_{y,2}\big) = \\ \varepsilon_y \sin\Omega t + \eta(t) \ . \end{aligned} \tag{13}$$

  The results of the simulation are presented in Fig. 15b.
- Both control systems are not self-excited and are driven by some external oscillatory force. In this case the phases may be also locked. This explanation seems to be rather unlikely, because in such a case the phases must be always entrained. The transitions between non-synchronous and

synchronous oscillatory patterns, or between different synchronous states would be impossible.

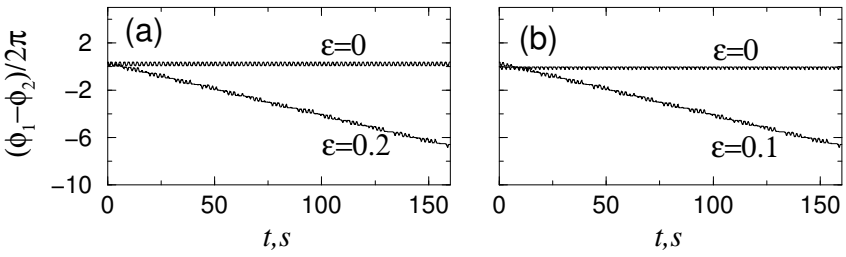

Fig. 15. (a): Mutual synchronization of two postural control systems (see 14a). In the absence of coupling ($\varepsilon_x = \varepsilon_y = \varepsilon = 0$) the phases diverge. Coupling $\varepsilon = 0.2$ leads to phase locking. (b): Synchronization of two control systems by a common external source. The parameters are: $\lambda_{x,1} = \lambda_{y,1} = 0.01$, $\lambda_{x,2} = \lambda_{y,2} = 0.05$, $c_{x,1} = 4$, $c_{x,2} = 8$, $c_{y,1} = 6$, $c_{y,2} = 8$, $\sigma_\xi = \sigma_\eta = 0.1$

We note that, as our goal was to demonstrate the phase synchronization properties of our model, we restricted our simulations to the case of a symmetric coupling only. Certainly, an asymmetric coupling seems to be more realistic. This was confirmed by calculation of higher order GMI functions $I_{\varepsilon,\vartheta}$. Obviously, synchronization can be observed in this case as well.

From the information available we cannot decide which of the described oscillatory structures is responsible for the phase locking observed in experiments. Certainly, different cases might be encountered in different physiological states. The understanding of physiological mechanisms leading to the appearance of the phase locking is a challenge for further investigations.

5 Conclusions

We have studied postural control in humans while quiet standing with open and closed eyes and with additional video–feedback. We have analyzed the interrelations between components of stabilograms using linear and nonlinear techniques. Our investigations demonstrate that in the healthy state the regulation of posture in anterior–posterior and lateral directions x and y can be considered as independent processes. This fact may be expected from the point of view of the control theory because independence of two control loops provides high reliability of a well operation of the whole system.

Further, we demonstrated that the occurrence of certain relationships between the x and y components of stabilograms can be revealed with the help

of the generalized mutual information functions and relative phase calculations. We hope that further developments of these techniques might result in the appearance of new diagnostic tools. The comparison of these methods of bivariate data analysis is also interesting in itself.

We have proposed a model of body sways in anterior–posterior and lateral direction. The model qualitatively describes the appearance of noisy and oscillatory patterns in stabilograms, and the arising of phase synchronization. We proposed two plausible oscillatory structures that can explain the observed effect of phase locking between x and y. A very interesting problem is to find out which of these mechanisms (or, perhaps, both) are responsible for the phase synchronization. Further experiments, in particular simultaneous measurement of EEG or/and disturbances of the posture may be helpful.

We believe that further theoretical and experimental studies of postural dynamics can provide better insight in the organization of human motor control, and thus it could help in the development of methods of differential diagnostics.

6 Acknowledgments

We thank P. Tass and A. Pikovsky for helpful comments. M. R. is grateful to the Alexander von Humboldt Foundation for financial support, and B. P. to the Deutsche Forschungsgemeinschaft supporting this work with the project Po442/2–1.

References

Aggashjan R., Pal'cev E. (1975): Reproduction of several special features of upright posture control in humans by means of a mathematical model. Biofizika **20**, 137–142

Baron J. (1983): History of posturography. In Igarashi M., Black F. (Eds.) (1983): *Vestibular and Visual Control of Posture and Locomotor Equilibrium.* Karger, Basel. pp. 54–59

Cernacek J. (1980): Stabilography in neurology. Agressologie **21D**, 25–29

Chow C., Collins J. (1995): A pinned polymer model of posture control. Phys. Rev. E **95**, 907–912

Collins J., De Luca C. (1994): Random walking during quiet standing. Phys. Rev. Lett. **73**, 764–767

Dobrynin S.A., Feldman M.S., Kuuz R.A., Firsov G.I. (1985): Analysis of trajectory of human center of gravity while standing in norm and pathology. In *Solving Mechanical Engineering Problems with Computers.* Nauka, Moscow. pp. 74–81

Feldman A.G. (1979): *Central and Reflex Mechanisms in the Control of Movement.* Nauka, Moscow

Firsov G.I., Rosenblum M.G., Landa P.S. (1993): Deterministic $1/f$ Fluctuations in Biomechanical System. In Handel P.H., Chung A.L. (Eds.) *Noise in Physical Systems and* $1/f$ *Fluctuations.* AIP Press, New York. pp. 716–719

Furman J. (1994): Posturography: uses and limitations. In: *Bailliére's Clinical Neurology* Vol. **3** Bailliére Tindall. pp. 501–513

Gurfinkel V., Kots Y., Shik M. (1965): *Regulation of Posture in Humans.* Nauka, Moscow

Gurfinkel V., Lipshits M., Popov K. (1982): Thresholds of kinestatic sensitivity in upright posture. Fiziologija Cheloveka **8**, 981–988

Hogan N. (1985): The mechanisms of multi-joint posture and movement control. Biol. Cybern. **52**, 315–331

Humprey D., Reed D. (1983): Separate cortical systems for control of joint stiffness: reciprocal activation and coactivation of antagonist muscles. In *Motor Control Mechanisms in Health and Disease.* Raven Press, New York. pp. 347–372

Lipp M., Longridge N. (1994): Computerized dynamic posturography: its place in the evaluation of patients with dizziness and imbalance. J. of Otolaryngology **23**, 177–183

Litvincev A., Tur I. (1988): Controlling muscle activity in a joint final position while performing simple movements. Fiziologija Cheloveka **14**, 539–545

Matsushira T., Yamashita K., Adachi H. (1983): A simple model to analyze drifting of the center of gravity. Agressologie **24**, 83–84

Pikovsky A.S., Rosenblum M.G., Kurths J. (1996): Synchronization in a population of globally coupled chaotic oscillators. Europhys. Lett. **34**, 165–170

Pompe B. (1993): Measuring statistical dependencies in a time series. J. Stat. Phys. **73**, 587–610

Rosenblum M.G., Feldman M.S., Firsov G.I., (1989): Investigation of the Biomechanical System. In *Methods and Software of Computer-Aided Experiment in Machine Dynamics.* Nauka, Moscow. pp. 259–277

Rosenblum M.G., Firsov G.I. (1992a): Stochastic self-oscillations in the system of human vertical posture control. I. Strategy of posture control and dynamical model. Biomechanics (Sofia) **24**, 34–41

Rosenblum M.G., Firsov G.I., (1992b): Stochastic self-oscillations in the system of human vertical posture control. II. Simulation and experiment. Biomechanics (Sofia) **25**, 37–43

Rosenblum M.G., Pikovsky A.S., Kurths J. (1996): Phase synchronization of chaotic oscillators. Phys. Rev. Lett. **76**, 1804–1807

Terekhov Y. (1976): Stabilometry as a diagnostic tool in clinical medicine. Canadian Med. J. **115**, 631–633

Williams W. (1981): A system oriented evaluation of the role of joint receptors and other afferents in position and motion sense. CRC Crit. Rev. in Biomed. Eng. **7**, 23–77

Yong J.B. (1994): Contour representation of sway area in posturography and its application. Archives of Physical Medicine and Rehabilitation **75**, 951–956